Biophysical Chemistry 42 (1992) 87–92
Elsevier Science Publishers B.V., Amsterdam

BIOCHE 01620

Fibrinogen adsorption on Pyrex glass tubes: A continuous kinetic study

F. Boumaza, Ph. Déjardin *, F. Yan, F. Bauduin and Y. Holl

Institut Charles Sadron (CRM-EAHP), CNRS-ULP 6, rue Boussingault, 67083 Strasbourg Cédex (France)

(Received 26 March 1991; accepted in revised form 14 June 1991)

Abstract

We present an experimental system to record continuously the adsorption kinetics of radiolabeled proteins, following an earlier study (Voegel et al., Colloids Surfaces 10 (1984) 9). We found results in accordance with the Lévêque equation at a wall shear rate of 50 s^{-1}, for adsorption from fibrinogen solutions in Tyrode's buffer on Pyrex glass tubes. Dependence on concentration in the range 4 to 200 $\mu g/mL$ and on distance to the tube entrance were examined. At the highest concentrations, a second slower regime appeared when coverage exceeded about 0.14 $\mu g/cm^2$.

Keywords: Fibrinogen adsorption; Adsorption kinetics on tubes

1. Introduction

In a previous publication [1], it was proposed to study the adsorption kinetics of proteins onto solid surfaces by recording continuously the radioactivity of a tube with a solution of labeled molecules flowing through it. This method should give essentially the same parameters as the more sophisticated Total Internal Reflection Fluorescence (TIRF) technique presented by Lok et al. [2], when used for flowing systems. One advantage of the radiolabeling technique is its suitability for study of adsorption phenomena on a large variety of tubing materials from glass to polymers. It does not require the preparation of flat surfaces. However, most experiments involving radiolabeled molecules give the amount adsorbed after rinsing with the solvent and therefore lead to a discontinuous study of the kinetics [3,4]. The rinsing procedure is justified by the so-called "irreversible" or metastable state of adsorbed proteins. Only a few papers relate continuous study of adsorption, desorption or exchange on beads packed into columns [5–7], or on the walls of a tube [1,8].

This study concerns phenomena occurring when blood contacts foreign materials, especially those intended to be biomaterials. It is believed that for most supports the first step to occur is the formation of a proteinaceous layer, since diffusion transport of proteins towards the surface occurs faster than transport of cells. Besides, protein adsorption is often found to be a partially reversible process [8], whose importance could

* To whom correspondence should be addressed.

depend on surface occupation [9] and residence time [10]. Hence, in order to gain some insight into the elementary processes leading to a final irreversibly adsorbed population, it appears essential to have some knowledge of the rate of transport of proteins from the bulk solution towards the surface. This can be achieved by using a slit [2,10,11] or tube [1,8] geometry. Then the hydrodynamic patterns are well known: the fluid velocity assumes a parabolic profile according to Poiseuille's law (laminar flow).

We present in this paper our experimental system used to follow the adsorption of fibrinogen onto Pyrex glass capillaries. Detailed study of the adsorption kinetics reveals a first Lévêque regime followed by a slower regime starting at a coverage of about 0.14 $\mu g/cm^2$.

2. Materials and methods

2.1 Experimental system

The experimental system is schematically represented in Fig. 1. A microcomputer controls two syringe pumps, one containing Tyrode's buffer, pH 7.35, the other a solution of fibrinogen at concentration C_b in the same buffer. Diversion towards a waste vessel is possible just before the flow enters the capillary to be examined, to eliminate air bubbles. The syringes are connected *via* teflon tubing to the 20 cm long glass capillary, of which the middle portion is positioned in front of a 5 cm diameter NaI detector. Lead walls limit the analysis to the 2 cm long part at the center of the detector. Data are visualized on a screen and stored in a microcomputer, each experimental point corresponding to the integrated radioactivity over 10 or 20 seconds. At the capillary exit the liquid is collected on a balance, from which the readings also appear graphically on the screen. Thus any disturbances in the flow line are instantaneously visualized.

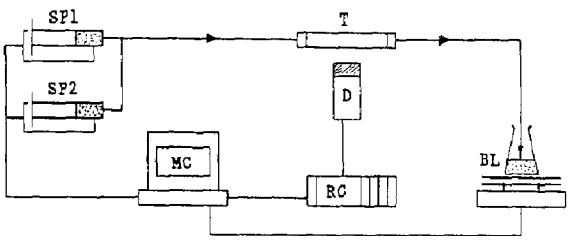

Fig. 1. Schematic drawing of the apparatus. A microcomputer (MC) controls two syringe pumps (SP1, SP2) and collects data from the radioactivity counter (RC) and from the balance (BL). The tube (T) under investigation is in front of a detector (D).

Flow rate was 4.6 mL/min, corresponding to a wall shear rate of 50 s^{-1}. We performed alternate flows of solution (10 min) and buffer. This period appeared to be too short to reach a stable value of adsorbance, while during rinsing with buffer a continuous slow decrease of the interfacial concentration Γ was observed.

2.2 Preparation of fibrinogen solutions

Human fibrinogen purified by the solvent/detergent technique was obtained from the Centre Régional deh Transfusion Sanguine de Strasbourg (CRTS, Strasbourg, France). The coagulability was 98% before and 95% after radiolabeling and fibronectin content < 5%. Concentrated Tyorde's buffer (160 g NaCl, 4 g KCl, 20 g $NaHCO_3$, 1.16 g $NaH_2PO_4 \cdot H_2O$, completed to one liter with (Super-Q Millipore) deionized water was filtered through 0.45 μm Millex filters before storing at +4 °C. Tyrode's buffer used for fibrinogen solutions was prepared just before experiments by dilution 1:20 in water and adjusted to pH 7.35 with 1 *M* HCl. Fibrinogen (1–5 mL, $C = 2$ mg/mL) was labeld by the iodogen technique [13] using $Na^{125}I$. Excess free iodine was removed by passage through an ion exchange resin preconditioned with Tyrode's buffer and 0.125–0.5 mL aliquots of the radiolabeled fibrinogen solution were stored at −18 °C. Quick thawed (37 °C) aliquots were then diluted with filtered buffer just before starting the experiments. There are possible artefacts involved in the use of iodine-labeled proteins, but is currently accepted that fibrinogen shows little physicochemical and biological alterations at low degree of iodination [14] as in this study. Using solutions with various percentage of labeled proteins shows no variation in the adsorbance on a variety of supports [15].

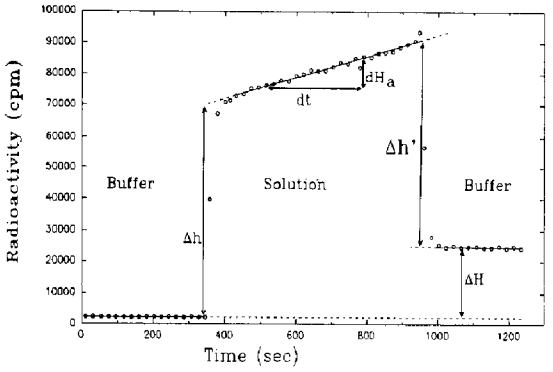

Fig. 2. Radioactivity recording ($C_b = 6.45$ μg/mL) showing the successive passages of buffer, solution and buffer.

2.3 Determination of fibrinogen adsorbance and apparent kinetic constants

We performed calibration *in situ* by estimation of the radioactivity change due to filling or emtying of the tube (radius R) with a solution of known concentration C_b. Schematic representation of an experimental curve is shown in Fig. 2. Given Δh the activity rise while filling the tube, which is equal to the activity drop $\Delta h'$ when rinsing starts, and ΔH the residual activity after rinsing (Fig. 2), we have:

$$\Gamma = 0.5RC_b(\Delta H/\Delta h) \quad (1)$$

and the apparent adsorption constant:

$$k_{exp} = C_b^{-1}(d\Gamma/dt) = (0.5R/\Delta h)/(dH_a/dt) \quad (2)$$

hence this procedure does not require independent measurement of the specific activity. Ratios of lengths on the graph lead directly to Γ and $d\Gamma/dt$ when R is known.

For small diameters, however, complications may arise from the fact that when the process is partially controlled by the transport of solute towards the interface, the activity rise Δh (or the drop $\Delta h'$) does not correspond to a tube entirely filled with a solution of concentration C_b, since concentration depletion occurs in the Nernst layer near the wall. The importance of the correction depends on the thickness of the depleted layer as compared to the tube radius and on the magnitude of the depletion, which is related to the intrinsic adsorption constant k_a. If we consider the extreme case of complete control of the kinetic process by transport to the interface, as in the Lévêque model [16], we find, by simulation in a tube of radius 1.25 mm, at 9 cm from the tube entrance, a lower limit of 0.93 for the correction factor f_c which should appear on the right hand of eqs. (1) and (2) when Δh does not correspond to a tube filled with solution of concentration C_b. Therefore we would expect a maximal overestimation of 7% for the adsorbance and kinetic constant.

Another difficulty could be the possibility of rapid adsorption during the filling step thus leading to erroneous calibration using Δh (Fig. 2). This can be avoided by looking at the activity drop $\Delta h'$ at the start of rinsing. Since it is sometimes difficult or impossible to distinguish between tube filling and the beginning of adsorption, whereas desorption occurs much more slowly than adsorption, calibration from the activity drop would appear to be more reliable and was actually used for data treatment.

At the highest concentrations we observed two successive regimes. Figure 3 represents such an experimental recording of activity versus time at $C_b = 13.1$ μg/mL. Full lines, continued by interrupted lines, show the linear fits of the data for adsorption and desorption steps. We arbitrarily defined the intercepts of these lines as points separating the successive regimes. The activity level corresponding to the total (background and calibration $\Delta h'$) is represented by a dotted line.

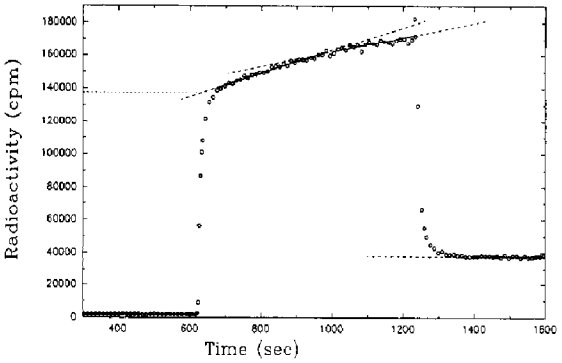

Fig. 3. Radiactivity versus time for adsorption from a fibrinogen solution at 13.1 μg/mL, showing two successive kinetic regimes.

This total was the zero level for calculation of the adsorbances.

2.4 Glass capillaries

The Pyrex capillaries of length 20 cm were about 4 mm external diameter and 2.50 mm internal diameter. They were cleaned using an ammonium persulfate/sulfuric acid mixture, rinsed with water and dried overnight in an oven at 40 °C.

3. Results and discussion

3.1 Adsorption kinetic constants

Table 1 summarizes the experimental kinetic constant k_{exp}, to be compared with the Lévêque constant $k_{Lev} = 3.22\ 10^{-5}$ cm s^{-1} calculated using diffusion coefficient $D = 2\ 10^{-7}$ cm^2 s^{-1}, shear rate $\gamma = 50$ s^{-1} and distance to the tube entrance $z = 9.3$ cm

$$k_{exp} = C_b^{-1}(d\Gamma/dt)_{exp} \quad (3)$$

$$k_{Lev} = C_b^{-1}(d\Gamma/dt)_{Lev} = 0.54 D^{2/3}\gamma^{1/3}z^{-1/3} \quad (4)$$

We observe good correlation between these two values. Therefore, at this shear rate, the process is essentially controlled by transport to the interface. Let us note that at the highest solution concentrations, we observed two successive regimes (Fig. 3). The crossover between the two regimes could be attributed to a decrease of the adsorption rate due to occupation of the surface, which would necesssitate reconformation and diffusion of molecules on the surface. Let us note that we neglected the entrance flow effect as the steady parabolic Hagen–Poiseuille flow is established actually at a small distance $L_e = 3.2$ mm from the tube entrance [17] in our experimental conditions thus leading to a negligible 1% correction in the estimation of k_{Lev}.

Table 1

Experimental apparent adsorption constant k_{exp} at various solution concentrations C_b. Adsorbance $\Gamma = \Gamma_1 + \Gamma_2$ at the end of the adsorption step. Desorption kinetic constant k_d.

C_b (μg/mL)	$k_{exp} \times 10^5$ (cm s^{-1})		$\Gamma = \Gamma_1 + \Gamma_2$ (μg/cm^2)	k_d (h^{-1})
	Regime 1	Regime 2		
4.35	3.19±0.11		0.092	0.24±0.27
6.45	3.22±0.11		0.137	0.22±0.17
9.00	3.24±0.13	2.38±0.19	0.130+0.053	0.10±0.16
13.1	3.21±0.10	2.04±0.37	0.138+0.080	0.10±0.07
19.4	3.22±0.22	2.76±0.22	0.123+0.237	0.83±0.15

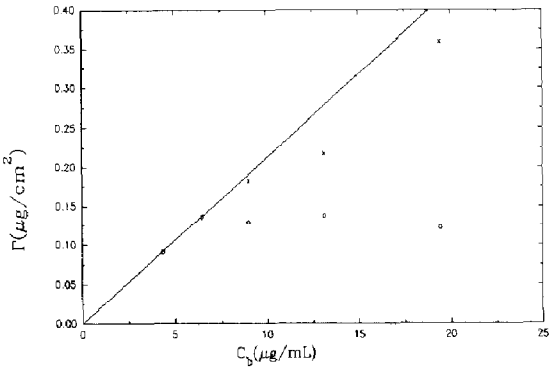

Fig. 4. Amount of fibrinogen adsorbed Γ versus solution concentration C_b after 10 minutes exposure to the solution at a shear rate of 50 s^{-1}. The open circles (○) denote Γ_1 and the crosses (×) $\Gamma_1 + \Gamma_2$.

3.2 Fibrinogen adsorbance

Figure 4 shows the variations of the interfacial concentrations Γ_1 and $\Gamma = \Gamma_1 + \Gamma_2$ with solution concentration C_b. Γ_1 is the adsorbance in the first fast regime while Γ_2 is the adsorbance in the second kinetic regime. We observe an increase of Γ with bulk concentration until values still largely below the saturation level of about 1.0 μg/cm^2 corresponding to the model of end-on adsorption [15]. The linear fit from the two smaller values gives an average value of 3.37 10^{-5} cm s^{-1} for the apparent kinetic constant, quite close to the theoretical Lévêque constant 3.22 10^{-5} cm s^{-1}. The amount of protein adsorbed in the first regime varies between 0.09 at the lowest concentration to an upper limit of 0.13–0.14 μg/cm^2. This limit should represent a crowded surface, where interactions between adsorbed molecules become important and surface exclusion effects are no longer negligible: the intrinsic adsorption rate at the surface becomes comparable to the transport rate and will later control significantly the kinetic process. It corresponds to the lowest

theoretical value for closed-packed side-on adsorption model, within the schematic representation of the conformationally unchanged fibrinogen molecule by a parallelepiped of dimensions $45 \times 9 \times 6$ nm^3. Such a value could, however, correspond also to a not so compact coverage with some population adsorbed end-on. Of course we cannot claim from this only result that fibrinogen is not denaturated at all in the adsorbed state.

3.3 Fibrinogen desorption

Table 1 shows the results for the slow desorption process. Linear variation of the recorded radioactivity throughout the 5 or 10 minute rinsing step leads directly to an estimation of the kinetic desorption constant k_d:

$$k_d = -\Gamma_e^{-1}(d\Gamma/dt) \qquad (5)$$

where Γ_e is the amount of protein adsorbed at the end of the adsorption step, as we assume that transport away from the interface is rapid compared to interfacial desorption. We observe significant desorption only for the highest surface concentration: this suggests that at high surface concentration a part of the surface population consists of loosely attached molecules, most probably the last to arrive, which could not optimize to a sufficient extent their interaction with the surface within a delay of a few minutes, because of the already largely occupied surface.

3.4 Influence of distance to the tube entrance

To confirm the conclusion of diffusion control, we performed an analysis along the tube, which can be done after the rinsing step. To check the Lévêque model (eq. 4), we represent in Fig. 5 the experimental quantity C_b^{-1} $(\Delta\Gamma/\Delta t)$ versus $z^{-1/3}$, where z is the distance from the tube entrance and $\Delta\Gamma$ the adsorbance after an adsorption time of Δt. As kinetic analysis reveals the existence of two regimes at the highest bulk concentrations, we can see that the data are roughly separated into two groups. Results relating to adsorption from these high bulk concentrations were disregarded in the distance analysis. For the three lower concentrations, we observe good superposition of the data at small $z^{-1/3}$, while some dispersion occurs at high $z^{-1/3}$, especially due to the 6.45 μg/mL experiment. Fit of the data to eq. (4) thus leads to a diffusion coefficient $D = 2.25\ 10^{-7}$ cm^2 s^{-1}, 10% higher than the theoretical value. We are however in accordance from this analysis with the conclusion of a kinetic process mainly controlled by the diffusion transport of molecules from the bulk solution towards the surface.

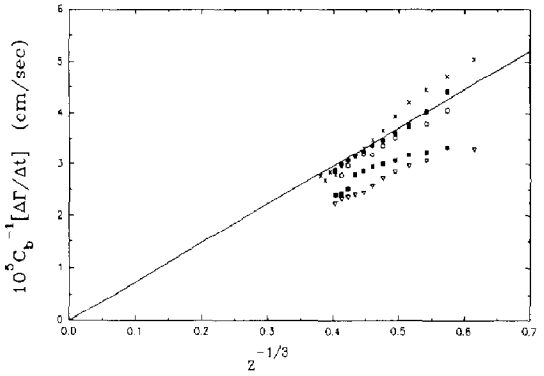

Fig. 5. C_b^{-1} $(\Delta\Gamma/\Delta t)$ versus $z^{-1/3}$ is the bulk solution concentration, $\Delta\Gamma$ the adsorbance after an exposure time of Δt and z the distance from the tube entrance. C_b (μg/mL) = 4.35 (○), 6.45 (×), 9.0 (●), 13.1 (▽), and 19.4 (■).

4. Conclusions

We showed that continuous kinetic analysis of the adsorption of fibrinogen on a glass tube is possible using radiolabeled fibrinogen. A critical interfacial concentration $\Gamma^* \simeq 0.14$ μg/cm^2 was determined, above which surface exclusion becomes important. Moreover, the kinetic diffusion control suggested by analysis at one particular point was confirmed by studying the adsorption along the tube, without being required to break it. These preliminary results indicate the possibility of determining the diffusion constant and reaction rate [18] from an analysis along the tube. However, such an analysis would necessitate measurements of the radioactivity closer to the tube entrance.

Acknowledgements

We are indebted to J. Mulvihill and J.P. Cazenave of the Centre Régional de Transfusion Sanguine dc Strasbourg for helpful discussions and for providing fibrinogen samples. Efficient technical assistance of J. Iss was fully appreciated. We also acknowledge the contribution of G. Maennel and F. Woehl for providing two syringe pumps.

References

1 J.C. Voegel, N. de Baillou, J. Sturm and A. Schmitt, Colloids Surfaces 10 (1984) 9.
2 B.K. Lok, Y.-L. Cheng and C.R. Robertson, J. Colloid Interface Sci. 91 (1983) 87.
3 S.M. Slack and T.A. Horbett, J. Colloid Interface Sci. 124 (1988) 535.
4 J.L. Brash and S. Uniyal, J. Polym. Sci. Polym. Symp. 66 (1979) 377.
5 N. de Baillou, J.C. Voegel and A. Schmitt, Colloids Surfaces 16 (1985) 271.
6 J.C. Voegel, N. de Baillou and A. Schmitt, Colloids Surfaces 16 (1985) 289.
7 J.C. Voegel, Ph. Déjardin, C. Strasser, N. de Baillou and A. Schmitt, Colloids Surfaces 25 (1987) 139.
8 J.L. Brash and Q.M. Samak, J. Colloid Interface Sci. 65 (1978) 495.
9 J.L. Brash, S. Uniyal, C. Pusineri and A. Schmitt, J. Colloid Interface Sci. 95 (1983) 28.
10 S.M. Slack and T.A. Horbett, J. Colloid Interface Sci. 133 (1989) 148.
11 Y.-L. Cheng, B.K. Lok and C.R. Robertson, in: Protein adsorption, ed. J. Andrade, Surface and interfacial aspects of biomedical polymers, Vol 2 (Plenum Press, new York, NY, 1985) p. 121.
12 E.W. Merrill, V.S. da Costa, E.W. Salzmann, D. Brier-Russell, L. Kuchner, D.F. Waugh, G. Trudel, S. Stopper and V. Vitale, in: Biomaterials: Interfacial phenomena and applications, eds. S.L. Cooper and N.A. Peppas (American Chemical Society, Washington, DC, 1982.)
13 E. Regoeczi, in: Iodine-labeled plasma proteins, vol. 1 (CRC Press, Boca Raton, FL 1984), p. 49.
14 B. Ly and P. Kierulf, Thromb. Res. 5 (1974) 327.
15 A. Schmitt, R. Varoqui, S. Uniyal, J.L. Brash and C. Pusineri, J. Colloid Interface Sci. 92 (1983) 25.
16 A. Lévêque, Ann. Mines 13 (1928) 284.
17 C. Fédiaevski, I. Voïtkouski and Y. Faddéev in: Mécanique des fluides (Mir, Moscou, 1974) p. 259.
18 Ph. Déjardin, J. Colloid Interface Sci. 133 (1989) 418.